Supplement of Atmos. Chem. Phys., 26, 8553–8573, 2026
https://doi.org/10.5194/acp-26-8553-2026-supplement

Atmospheric Chemistry and Physics
Open Access
EGU

Supplement of

Decomposing pre-industrial to present-day land use change forcing in the UK Earth System Model

Emma Sands et al.

Correspondence to: Emma Sands (e.g.sands@ed.ac.uk)

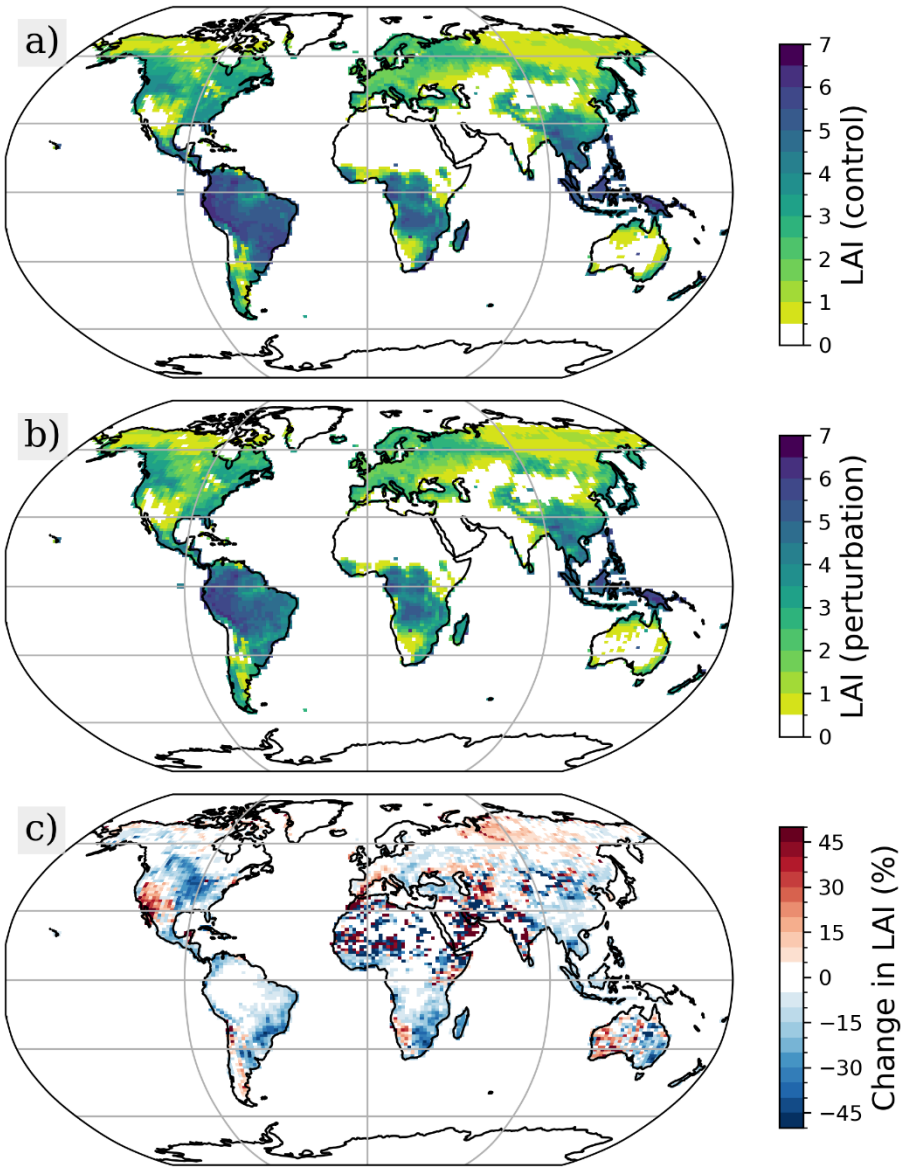

Figure S1. Leaf Area Index (LAI) for 1850 control (a) and present-day perturbation (b). Panel (c) shows the change from pre-industrial to present-day conditions (2014 – 1850) as a % of the 1850 LAI.

Table S1. Sulfate aerosol formation fluxes under pre-industrial conditions and response to the land cover perturbation.

Secondary SU production	Standard chemistry		Complex chemistry	
	Pre-industrial (Tg(S) yr^{-1})	Change in land cover perturbation (%)	Pre-industrial (Tg(S) yr^{-1})	Change in land cover perturbation (%)
Nucleation via OH	0.03 ± 0.00	+3	0.02 ± 0.00	+6
Condensation via OH	7.09 ± 0.01	+4	6.92 ± 0.01	+2
In-cloud via H_2O_2	5.31 ± 0.01	-3	3.65 ± 0.01	-3
In-cloud via O_3	1.13 ± 0.00	0	0.58 ± 0.00	+2

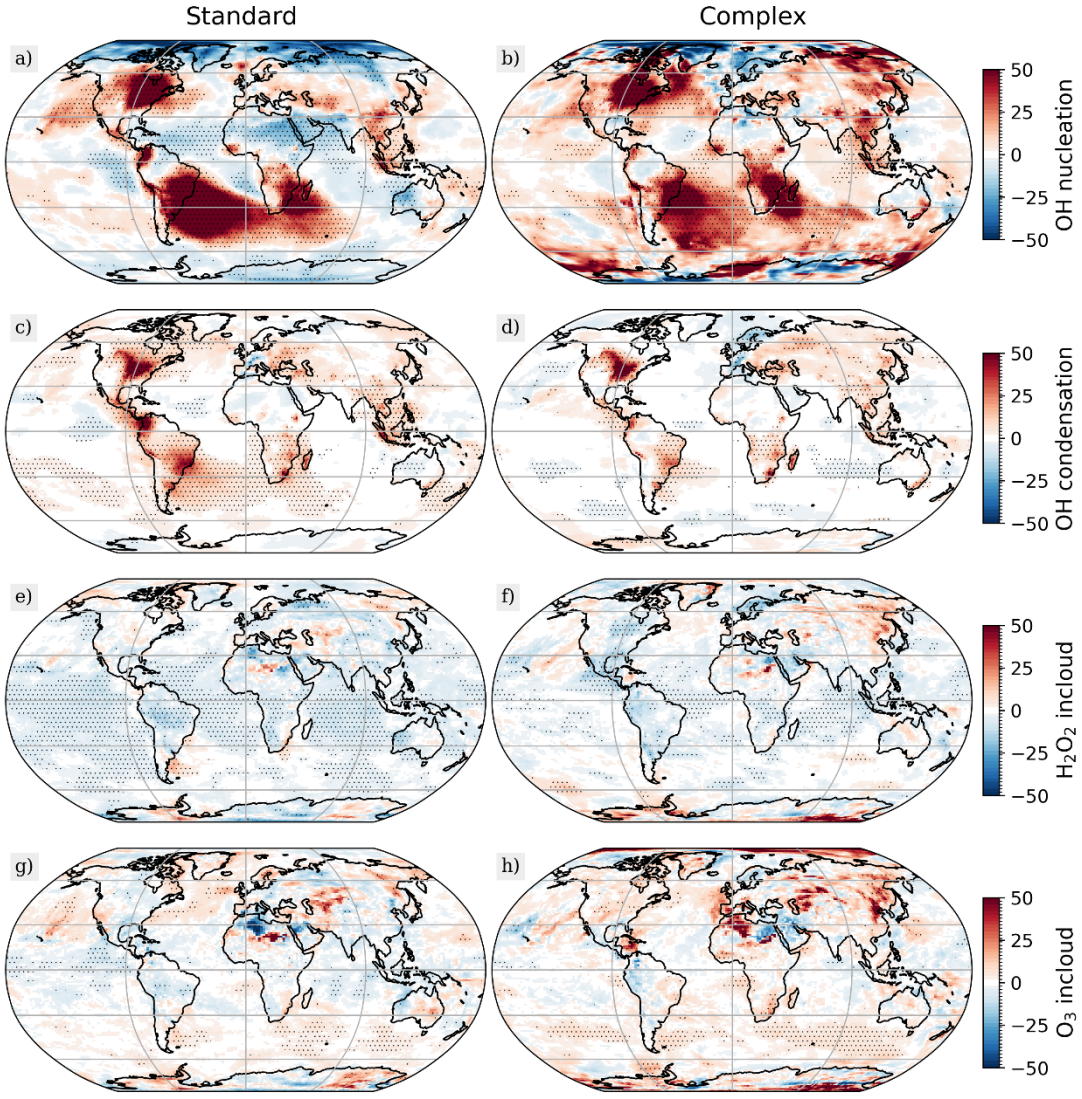

Figure S2. Changes (%) in sulfate aerosol formation fluxes for the standards (left column) and complex (right column) chemistry mechanisms in response to pre-industrial to present-day land cover change. The aerosol formation is divided in to nucleation with OH (a, b), condensation with OH (c, d), in-cloud reactions with H_2O_2 (e, f), and in-cloud reactions with O_3 (g, h).

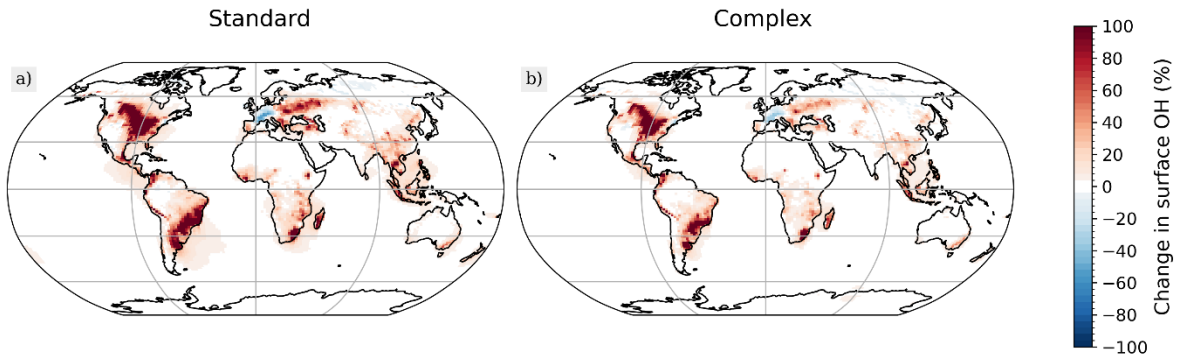

Figure S3. Change in surface OH in response to pre-industrial to present-day land use change for the standard (a) and complex (b) chemistry mechanisms.

Table S2. Regional mean radiative forcing values from pre-industrial to present-day land use change.

Region	Forest cover (%)	Grass cover (%)	Isoprene emissions (%)		Monoterpene emissions		ERF_{LU} (W m^{-2})		IRF_{ARI}		ΔCRE		IRF_{O3}		RF_{alb}
Non-Arctic Ocean	0	+4	-1	0	0	0	0.02±0.06	0.05±0.05	0.04±0.02	0.04±0.01	0.02±0.04	0.04±0.04	-0.01±0.01	-0.02±0.01	0.01±0.01
USA and Canada	-17	+33	-16	-18	-18	-18	-1.20±0.11	-0.92±0.11	0.13±0.02	0.12±0.01	0.50±0.17	0.91±0.18	0.05±0.03	0.03±0.03	-2.19±0.14
Europe	+15478	+8	+172	+166	+133	123	-0.44±0.19	-1.03±0.22	0.08±0.03	0.09±0.03	0.11±0.24	-0.86±0.30	0.04±0.03	0.01±0.04	-0.65±0.19
South Asia	-8	+1723	-17	-16	-2	-2	0.08±0.30	-0.10±0.20	-0.01±0.06	0.07±0.06	0.26±0.11	-0.11±0.12	0.01±0.02	-0.02±0.02	-0.29±0.17
East Asia	-6	+22	-15	-14	-7	-9	0.00±0.15	-0.21±0.15	0.03±0.04	0.07±0.03	0.78±0.19	0.24±0.22	0.02±0.03	0.01±0.03	-0.37±0.08
Southeast Asia	-17	+74	-20	-19	-17	-18	-0.33±0.17	-0.43±0.14	0.16±0.02	0.21±0.02	0.66±0.12	0.33±0.18	-0.01±0.02	-0.01±0.01	-0.96±0.03
Australia/Oceania	-7	+10	-6	-10	-3	-3	-0.01±0.18	0.11±0.16	0.04±0.04	0.04±0.03	-0.09±0.34	-0.01±0.32	-0.01±0.03	-0.02±0.02	-0.04±0.14
Northern Africa	-1	+1373	-1	-2	0	0	-0.07±0.25	-0.24±0.21	0.08±0.03	0.12±0.04	0.03±0.11	0.00±0.10	-0.01±0.02	-0.02±0.02	-0.03±0.09
Sub Sahel Africa	-16	+83	-22	-22	-13	-13	-0.09±0.13	-0.10±0.12	0.25±0.07	0.22±0.05	0.23±0.10	0.36±0.10	-0.01±0.01	-0.02±0.01	-0.27±0.05
Middle East	-3	+560	+3	+4	-1	-1	0.05±0.31	-0.37±0.24	0.09±0.03	0.04±0.03	0.23±0.13	-0.20±0.12	0.00±0.03	-0.03±0.03	0.11±0.12
Central America	-16	+206	-14	-15	-13	-13	-0.50±0.16	-0.70±0.16	0.07±0.02	0.10±0.02	0.33±0.12	0.33±0.12	-0.01±0.01	-0.01±0.01	-0.87±0.03
South America	-12	+93	-16	-16	-13	-14	-0.57±0.10	-0.52±0.11	0.15±0.01	0.19±0.02	0.72±0.13	0.60±0.12	0.00±0.01	-0.02±0.01	-1.05±0.03
Ukraine and Russia	-15	+12	-13	-16	-12	-14	-0.55±0.16	-1.11±0.20	0.12±0.02	0.11±0.02	0.31±0.18	-0.16±0.20	0.02±0.03	0.00±0.03	-0.99±0.21
Central Asia	+26	+6	+1	+1	-1	-1	-0.06±0.21	-0.09±0.21	0.12±0.06	0.03±0.06	0.04±0.27	0.16±0.19	0.03±0.03	-0.01±0.04	-0.80±0.33
Arctic	0	+21	0	0	1	0	-0.17±0.15	-0.11±0.15	0.02±0.01	0.03±0.02	-0.18±0.10	0.11±0.11	0.01±0.04	0.00±0.04	0.03±0.07
Antarctic	0	0	0	0	0	0	0.03±0.13	-0.38±0.15	0.01±0.00	0.01±0.00	-0.07±0.04	-0.06±0.07	0.00±0.02	-0.06±0.02	0.01±0.01

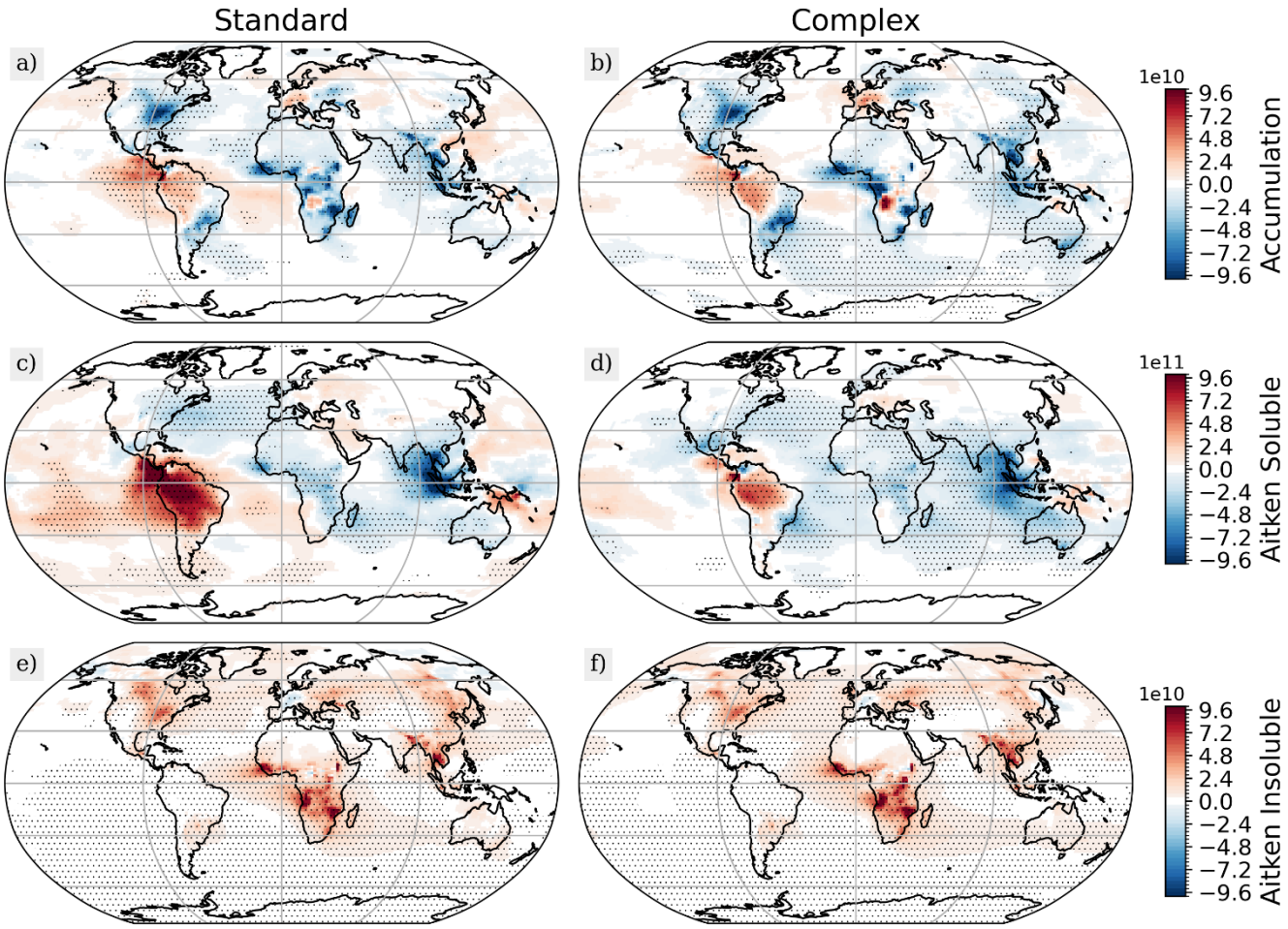

Figure S4. Change in accumulation mode (a,b), Aitken soluble mode (c,d) and Aitken insoluble mode (e,f) aerosol numbers (number m^{-2}) in response to pre-industrial to present-day land use change for the standard (left column) and complex (right column) chemistry mechanisms.

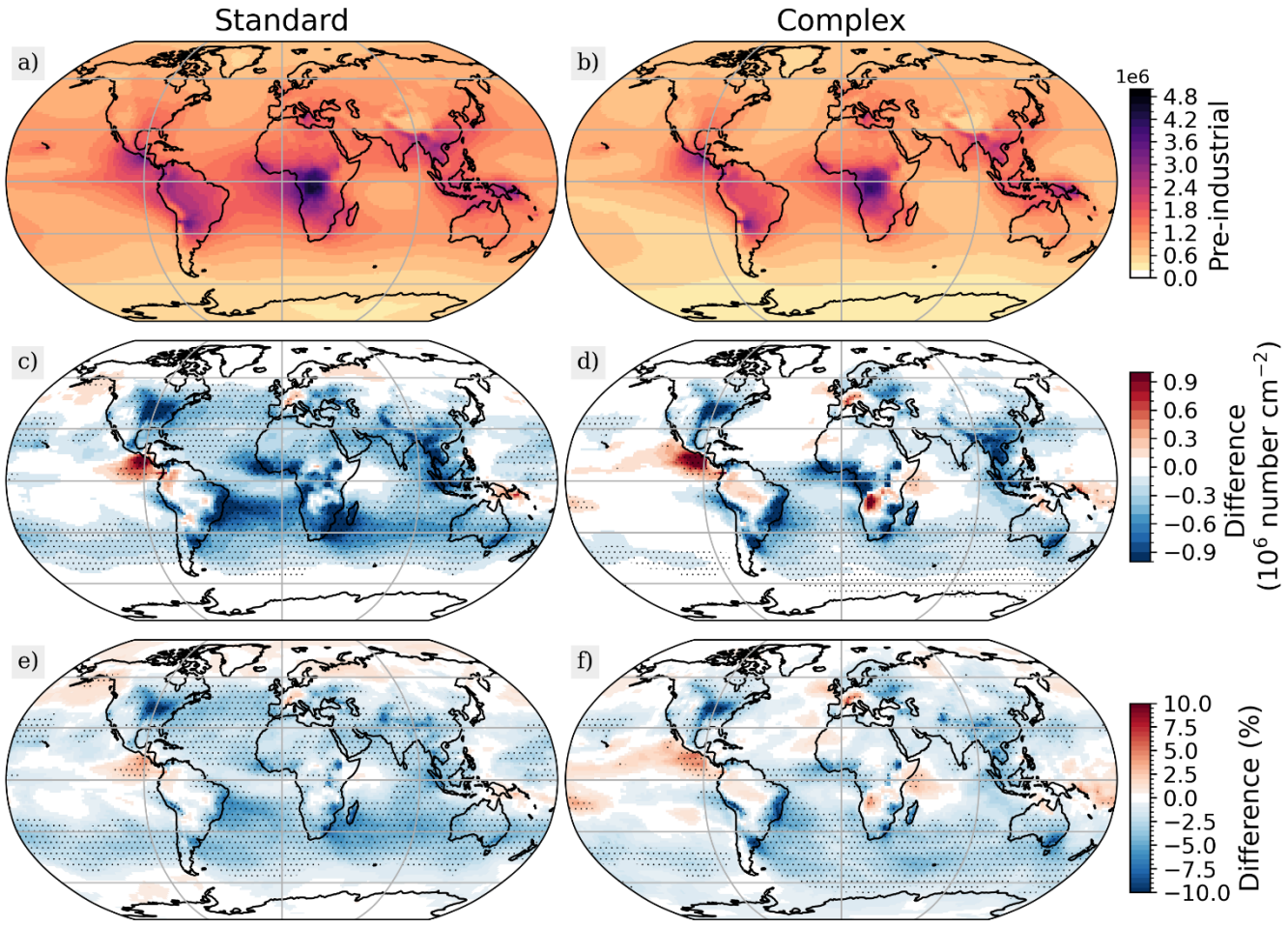

Figure S5. Cloud condensation nuclei (CNN) in the pre-industrial (a,b) and the change in CNN in response to pre-industrial to present-day land use change (c-f) for the standard (left column) and complex (right column) chemistry mechanisms.

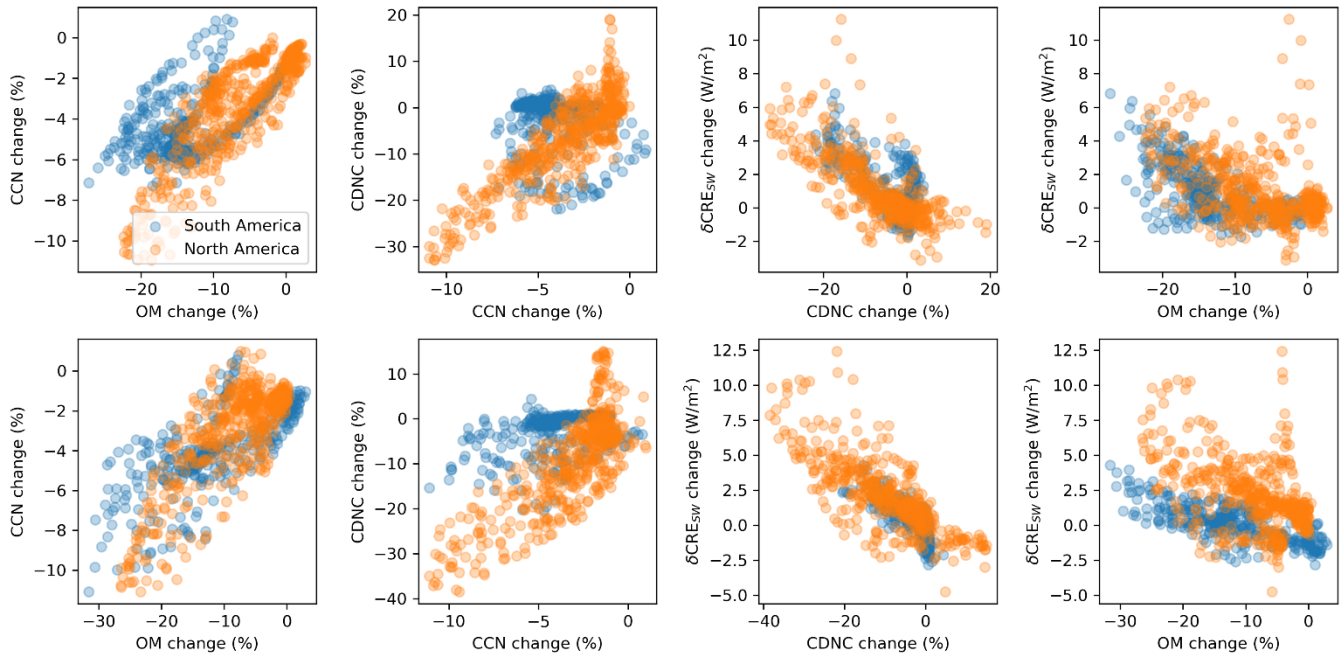

Figure S6. Connection between organic matter aerosol burden and change in shortwave cloud radiative effect through impacts on CCN and cloud droplet number concentration (CDNC). The top for shows results for the standard chemistry mechanism, while the bottom row refers to the complex chemistry mechanism.